

Article

An Analysis of Nanoparticles Derived from Coal Fly Ash Incorporated into Concrete

Alcindo Neckel ^{1,*} , Diana Pinto ², Bashir Adelodun ^{3,4}  and Guilherme L. Dotto ⁵¹ Faculdade Meridional, IMED, 304, Passo Fundo 99070-220, Brazil² Department of Civil and Environmental Engineering, Universidad de la Costa, CUC, Calle 58 # 55–66, Barranquilla 50366, Colombia; dpinto3@cuc.edu.co³ Department of Agricultural and Civil Engineering, Kyungpook National University, Daegu 41566, Korea; adbash2008@gmail.com⁴ Department of Agricultural and Biosystems Engineering, University of Ilorin, PMB 1515, Ilorin 240103, Nigeria⁵ Chemical Engineering Department, Federal University of Santa Maria, UFSM, 1000, Roraima Avenue, Santa Maria 97105-900, Brazil; guilherme_dotto@yahoo.com.br

* Correspondence: alcindo.neckel@imed.edu.br

Abstract: The environmental benefits of incorporating coal fly ash (CFA) into the concrete manufacturing process as a partial substitute for Portland cement are well known. What is less studied is the potential release of CFA derived nanomineral and amorphous nanoparticles during this process of incorporation. A thorough understanding of this makes it possible to understand the risks of exposure to particulates that are harmful to human health when CFA is mixed into concrete. The general objective of this study is to analyze airborne particulates released when CFA is mixed into concrete at the point of manufacture, focusing on the levels of nanominerals, amorphous nanoparticles and hazardous elements (HEs) contained within that are considered harmful to human health. These airborne particulates can be easily inhaled by plant workers in the absence of personal protective equipment. The authors analyzed samples of ash itself and collected actual airborne particulates using self-made passive samplers installed at the manufacturing plant. Regarding the ash analyzed, iron (Fe) was found in large amounts in relation to calcium (Ca), magnesium (Mg) and silicon (Si). The transport, disposal and application of CFA in civil construction projects can provide an increased efficiency and reduce overall costs associated with the production of concrete. However, CFA poses a threat to human health due to the significant amount of HEs, nanominerals, and amorphous nanoparticles found to be released into the environment at the manufacturing plant.

Keywords: coal fly ash; Al–Ca–Fe–Mg–Si spheres; mineralogy; complex structure; future projects



Citation: Neckel, A.; Pinto, D.; Adelodun, B.; Dotto, G.L. An Analysis of Nanoparticles Derived from Coal Fly Ash Incorporated into Concrete. *Sustainability* **2022**, *14*, 3943. <https://doi.org/10.3390/su14073943>

Academic Editors: Seungjun Roh and Marc A. Rosen

Received: 12 January 2022

Accepted: 24 March 2022

Published: 26 March 2022

Publisher's Note: MDPI stays neutral with regard to jurisdictional claims in published maps and institutional affiliations.



Copyright: © 2022 by the authors. Licensee MDPI, Basel, Switzerland. This article is an open access article distributed under the terms and conditions of the Creative Commons Attribution (CC BY) license (<https://creativecommons.org/licenses/by/4.0/>).

1. Introduction

Brazil has an abundance of coal reserves, estimated at approximately 11.1 billion tons [1]. Coal fired power plants exist in the Brazilian states of Rio Grande do Sul, Santa Catarina and Paraná, which together produce approximately 11% of the electricity produced in the entire country [2]. Thermoelectric power plants that utilize coal generate high amounts of inorganic residues, such as coal fly ash (CFA). Together with the desulfurization of combustion gases that are released into the atmosphere, these plants have negative impacts on local air quality and on the health of the population that resides in close proximity to the power plant [3]. The ash generated by burning coal has very few industrial uses and is generally treated as a waste product, thereby leading to environmental problems [3]. The physical process of combustion accumulates high concentrations of hazardous elements with metalloids within the coal ash, including: polycyclic aromatic hydrocarbons (PAHs), elemental carbon, fluorides, amorphous silica and aggregates to ultra fine particulate materials [4]. It is reported that the global annual production of

coal ash is approximately 600 million tons, and CFA accounts for approximately 80% of pollution on a global scale [5]. Only 20% of the fly ash is used in some way, while the remaining 80% is simply discarded [6]. Coal fly ash itself consists of pozzolanic material, which first began to be used in the 1950s and 1960s in the manufacture of concrete [7]. CFA is typically polymineralic and chemically complex [4]. Compared to ordinary Portland cement (OPC), the ash generated from burning coal has advantages related to the heat of hydration, facilitating the manufacture of byproducts, such as concrete, with greater strength and higher durability, in addition to lowering concrete manufacturing costs [8,9]. Several factors influence the chemical and physical properties and composition of coal fly ash [9]. Among other factors, of primary consideration is the type of coal burned. Furthermore, different combustion temperatures result in variations in the generated particle density [10].

Concrete is one of the most extensively utilized building materials in civil construction, on a global scale [11,12]. The addition of CFA to concrete generates nanoconcrete, with high density and superior performance, capable of supporting large loads in structures in civil construction [12,13]. Coal fly ash is not a perfect substitute for Portland cement, and it is only possible to displace between 15 and 75% of the Portland cement used in traditional concrete by substituting CFA in its place [13].

The utilization of CFA in the production of concrete is an example of industrial recycling [7]. Many works report the benefits of incorporating different types of CFA that can be used in concrete as a cement replacement [7,13,14]. In order to reduce direct impacts on the environment, the use of alternative materials, such as CFA for cement, would be considered useful. As a result, strategies aimed at the manufacturing of sustainable concrete to favor the reduction in harmful environmental impacts are highly desired [15]. The benefits of incorporating CFA into concrete could lead to the potential reduction in nanomineral and amorphous nanoparticles released to the environment during and following disposal [16]. However, this study examines the particles released to the environment as the CFA is mixed into concrete at the manufacturing plant.

The generation of carbonaceous matter and amorphous minerals in coal fired power plants is characterized as ultrafine particles or nanoparticles, ranging in size from 1 to 100 nm. Particulates of this size are potentially harmful to human health [8,14]. The vast majority of these ultrafine (<100 nm) and nanometric (<50 nm) particles are easily absorbed by the human body through the respiratory and digestive systems, even through the skin, thus compromising the health of the population [4]. Ultrafine particles and nanoparticles have high reactivity when compared to other particles, which have an increased volumetric surface [4]. More in depth knowledge on the nanomineral and amorphous nanoparticles that are generated from the reuse of CFA becomes of fundamental importance for the concrete manufacturing industry, in order to determine reliable risk assessment [17–19]. Currently, one of the main environmental and human health risks associated with the production of conventional concrete is the transportation of OPC and direct exposure resulting from the imprudent application of concrete without using personal protective equipment. This study examines the health risks to workers who mix CFA into cement during its manufacturing.

This study presents an exhaustive combination of multianalytical techniques to provide the most effective ways in which to utilize CFA produced by Brazilian thermoelectric power plants in concrete utilized for civil construction projects. We examine the composition of geochemistry in the spheres, and the forms of nanoparticles present in actual workplace emissions. The general objective of this study is to examine the characteristics of nanoparticles emitted as CFA is mixed with uncured concrete. We focus on understanding the levels of airborne nanominerals, amorphous nanoparticles and hazardous elements (HEs) contained within CFA dust that are considered harmful to human health. Considering the sustainability factors in repurposing CFA for use in civil construction through their incorporation into the manufacture of concrete, this study indicates the presence of elements dangerous to human health in the form of nanoparticles and ultra fine particles

suspended in the air during concrete manufacturing. This allows for a greater awareness of society regarding the need to create future measures that guarantee the protection of workers exposed during the concrete manufacturing process, if this practice is to be labeled truly sustainable.

2. Materials and Methods

Five self-made passive sampling devices were utilized for this study. Constructed of synthetic plastic polymers (PVC), the samplers offered external protection from adverse elements that could compromise the experiment, such as rain and strong winds, among others. In each PVC sampler a circular piece of foam, measuring 6 cm by 1 cm, was attached, necessary for the capture of particulates and ultra fine particles [20,21]. Thus, five passive samplers were installed at a level of 185.6 to 170.7 cm above the ground, the average height of the noses and mouths of the employees employed at the concrete company where sampling took place, thereby sampling realistic levels of particles the employees would likely inhale in the absence of personal protective equipment. The source of the CFA used at this concrete plant was the Capirovarí Coal Plant (Santa Catarina, Brazil). Each of the SMPSs was sampled in triplicate. Sampling methodology was carried out according to Oliveira et al. [21] and Trejos et al. [21]. Through each SMPS sampled, 80 particles were studied, selected to identify the chemical elements present in the collected material. Thermodynamics stands out, with CFA requiring between three to five days to stabilize at room temperature after leaving the boiler [19]. After five days of concrete manufacture, the particulate material from the fixed samplers was collected and properly stored in sterilized glass containers, isolated in a thermal styrofoam box, and immediately submitted for analysis to the Environmental Chemistry laboratory of Universidad de La Costa—CUC located in the city of Barranquilla, Colombia.

The analytic laboratory procedures were completed as outlined in Martinello et al. [4], Silva et al. [22], and Quispe et al. [23], which served as a methodological basis for the analysis of the material collected in the samplers, responsible for the collection of nanoparticles and ultra fine particles. For the analysis of the morphology and size of the samples collected at the concrete manufacturing site, FE-SEM (scanning electron microscope) and HR-TEM (high resolution transmission electron microscopy) were used, and applied to electron diffraction (SAED) [4,22]. The test parameters applied assigned nanoparticles, which include EDS (energy dispersive X-ray spectroscopy), coupled with FE-SEM and HRTEM, generating secondary electronic images of the surface of nanoparticles, with high resolutions [13]. The sample holders (HR-TEM) used in the collection of the material were cleaned to avoid contamination with a Gatan Model 950 plasma system. In addition, microbeam diffraction (MBD) was used in this study, which facilitated a detailed analysis along with the application of scanning transmission electron microscopy (STEM) [23,24]. For the STEM mapping, a drift correction system was used. The electron backscattered detector (BSE) mode was used because it presents greater efficiency in the analysis of the refining capacity of the atomic weight of the molecules processed in this study. For the topographic characterization of the surfaces of the particles, a secondary electron detector mode was used. For a high resolution image, fast Fourier transformation (FFT) was applied, resulting in a diffraction pattern that contains the same structural information as a SAED diffraction pattern. Sequential extraction and magnetic separation were applied [25]. In order to obtain composition information, a dual ion beam (FIB) of the FEI-DualBeam™ Helios 600 Nanolab™, high resolution emission (FEG) for SEM [26–29], trimmed by lens detectors (TLD), Everhart—Thornley (ETD) and electron backscattered (BSED) were used in this study [30–32]. Finally, a high resolution focused Ga⁺ ion beam to select [33–36], cut, and obtain an accurate image of a specific region of the species of interest, within the range of 100 nm, was also used [37–41]. These similar analytical procedures have been previously reported by several authors [21,23,42–51], especially with regard to necessary care that must be taken with the sampled material to avoid its contamination in the laboratory. This facilitated greater reliability of samples and results generated in this study.

3. Results and Discussion

The reused waste, CFA, is characterized as a substitute for OPC [7,12,14]. Coal byproducts at coal fired power plants and cement plants produce pulverized materials, which are also known as nanoparticles. The raw materials for Brazilian OPC production are imported into the country and transported from various locations to the manufacturing plants in several states. According to the proportions of the materials used, transport distances for different CFAs are considered. CFA, limestone, iron ore, sandstone, clay and gypsum are considered the main constituents of OPC [7,12,14].

Through the chemical samples analyzed, the presence of high levels of iron, silica and aluminum was observed [52]. It should be noted that both the CFA and calcium aluminate cement (CAC) are composed of vaporized material. However, the ash, which results from the burning of high levels of combustion gases in a thermoelectric power plant, is of lower density. Therefore, there is a greater dispersion of nanoparticles and ultra fine particles aggregated in a spherical shape when it is used, as shown by the results of the FE-SEM and HR-TEM analyses (Figure 1A,B). The presence of hazardous elements (HEs), such as boron (B), cadmium (Cd), chrome (Cr), fluorine (F), mercury (Hg) and lead (Pb), concentrated in CFAs were also observed, which are extremely dangerous both for the environment and for the health of the population.

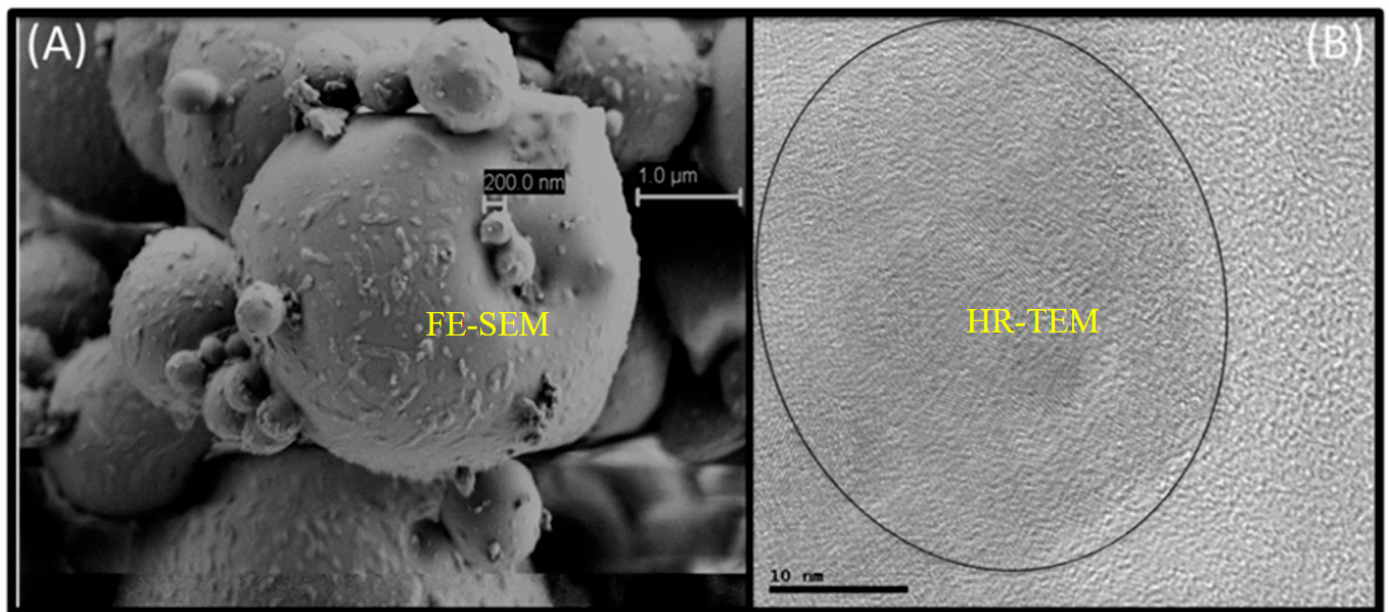


Figure 1. (A) FE-SEM images of the spheres and cenospheres and (B) HR-TEM image.

The results of this study confirm the findings by Teixeira et al. [7], Harihanandh et al. [12] and Babu et al. [14], that the use of CFA in the manufacture of concrete becomes an innovative and technological practice, benefiting the environment. The utilization of this waste product produced by coal fired power plants prevents it from being deposited in open air landfills, the current disposal method utilized in Brazil and most of the world for CFA.

The CFA and, consequently, the manufactured concrete are classified as having low bulk density, with a high capacity to retain H₂O and are of a neutral pH. The higher the percentage of ash applied, the greater the removal of harmful contaminants from the environment, thus preventing soil pollution by metallic elements [53]. HE contamination of soils by both coal and cement production and transportation presents a serious threat not only to the environment but also to human health [24,25]. It is known that CFA causes contamination that can affect various regions following irresponsible disposal of this industrial waste [54–58].

Specific Properties of Sampled CAC

Silva and Boit [16] reported that, in Santa Catarina, CFA presented twice as much quartz when compared to other analytical studies. Although it does not have an ultra fine density pattern, the molecular structure of nanoquartz detected in CAC (Figure 2) relates to the molecular structure of other pollutants present in the air. The observed nanosilica (Figure 2A) and ultrafine silicates (Figure 2B) are usually formed by high density particles, have smooth surfaces, and are generally spherical in shape with sharp edges. Thus, it is noteworthy that, in the analyzed material, the presence of single particles with high size aggregates contain silicate and ultra fines, thus forming nanoparticles with carbon characteristics (Figure 2). As observed from Figure 2B, the EDS spectrum for ultrafine silicates shows a high concentration of silicon (Si), aluminum (Al), carbon (C) and potassium (K), and a small proportion of sulfur (S), titanium (Ti), iron (Fe), sodium (Na) and chlorine (Cl). These elements can be harmful to human health.

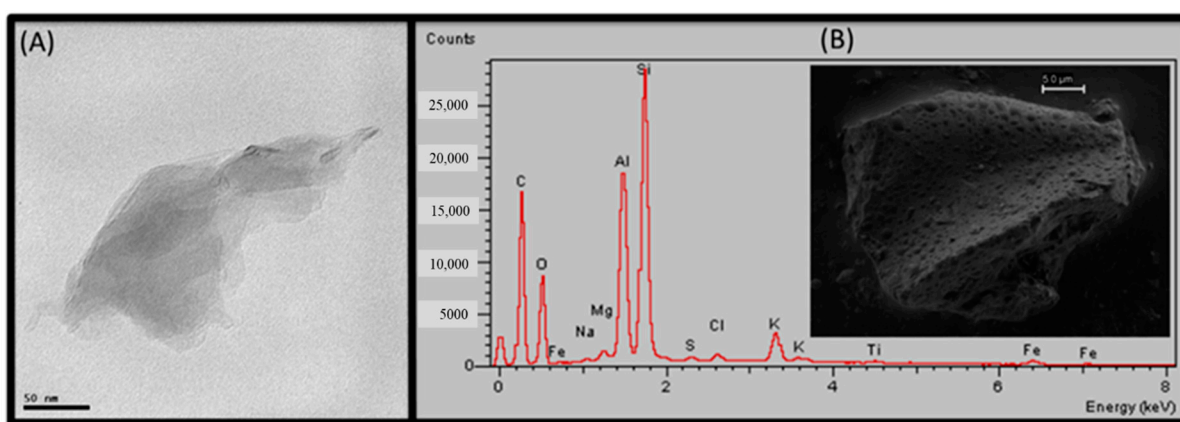


Figure 2. Ultrafine/nanoquartz in CAC. (A) Nanosilica, (B) ultrafine silicates including the EDS spectrum for elemental composition.

These results demonstrate a high amount of quartz in the analyzed samples, when compared to other studies [59,60]. In regions with a higher concentration of quartz in coal, cancer rates in the respiratory system of the population are higher. Thus, it is important to investigate the health implication of crystalline silica (quartz) on a global scale [59,61,62]. The use of CFA to manufacture concrete, reported in this study, can present a risk to human health due to exposure to certain particles by workers who either do not make adequate use of or are not supplied with personal protective equipment (gloves, goggles and facemasks with filters).

CFA is produced as a byproduct of burning coal that is crushed and ground to a fineness of 70–80%, passing through a 75 mm sieve (No. 200). An estimated 10–12% of it is used in producing concrete and concrete products [63,64]. Figure 3 shows the presence of nanoparticles and ultra fine particles collected by the samplers during the manufacture of concrete with the addition of ash. According to the literature, in a temperature range of 400–1000 °C, active progressions occur, such as the elimination of volatile elements dangerous to the environment and human health. This forms oxidizing reactions of sulfides, dehydroxylation of hydromics and carbonates (Figure 3A) [65,66]. The Fe phases identified in Figure 3C can originate from chemical reactions during the burning of mineral coal, forming ultra fine particles in the crystalline phases as a byproduct of the pyrite of the Fe sulfides [67,68], which was present in the analyzed samples. Goethite, magemite, magnetite and hematite, all interacting with clay minerals, formed an aluminosilicate glass, with amorphous characteristics, containing iron [67,68].

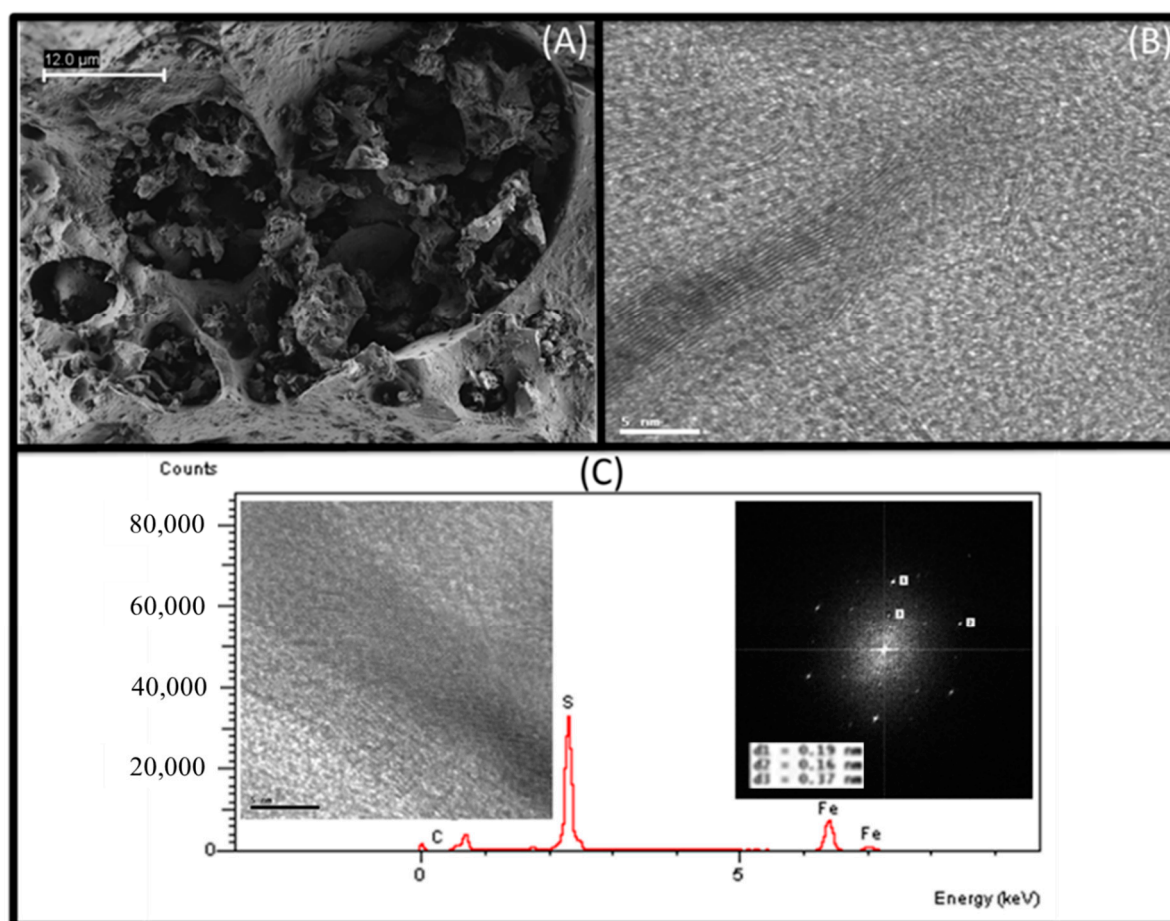


Figure 3. The traditional ultrafine/nanoparticles of cement detected in the present study. (A) Formation by the elimination of hazardous volatile matters from the coal, (B) HR-TEM image, and (C) HR-TEM images and FFT of nanopyrite including the EDS spectrum.

Figure 4 shows the detected spheres in CAC composed of Al–Ca–Fe–Mg–Si–Zr (zirconium). The spheres are relatively small in size (approximately 4.0–6.0 μm), mostly with spherical characteristics, a homogeneous surface, containing Al, Si and O and probably a glassy aluminosilicate matrix. These microspheres are the result of thermo-geochemical conversions, which originate through burning, mineral forms with Fe, or from the original coal. The burning of coal occurs at high temperatures, above 1200 $^{\circ}\text{C}$, using an oven in boilers, at 1200–1450 $^{\circ}\text{C}$, and the removal of ash occurs at a temperature of 1400–1700 $^{\circ}\text{C}$ in boilers, during the coal combustion process [69]. Meanwhile, during this burning process, the contaminants present in the coal can be released into the atmosphere, or become concentrated in the ash, both ultra fine elements can compromise the environment and human health.

Under the conditions of high temperatures in a reducing medium, the element Fe has the molecular format of Fe^{2+} , which may allow the formation of eutectics, with lower temperatures compared to Al–Ca–Fe–Mg–Si. Iron in the spheres (observed in the spectrum in small proportions, see Figure 4) can be associated with pyrite (FeS_2) in the composition of coal, being able to evolve into pyritic Fe during the heating of coal in thermoelectric plants [68]. In this relationship, iron sulphide minerals such as pyrrhotite ($\text{Fe}(1-x)\text{S}$), marcasite (FeS_2) and Fe sulphates such as rozenite ($\text{FeSO}_4 \cdot 4\text{H}_2\text{O}$), melanterite ($\text{FeSO}_4 \cdot 7\text{H}_2\text{O}$), roemerite [$\text{FeSO}_4 \cdot \text{Fe}_2(\text{SO}_4)_3 \cdot 14\text{H}_2\text{O}$], szomolnokite ($\text{FeSO}_4 \cdot \text{H}_2\text{O}$) and halotriquite [$\text{FeAl}_2(\text{SO}_4)_4 \cdot 22\text{H}_2\text{O}$] are found in the mineral properties of coal.

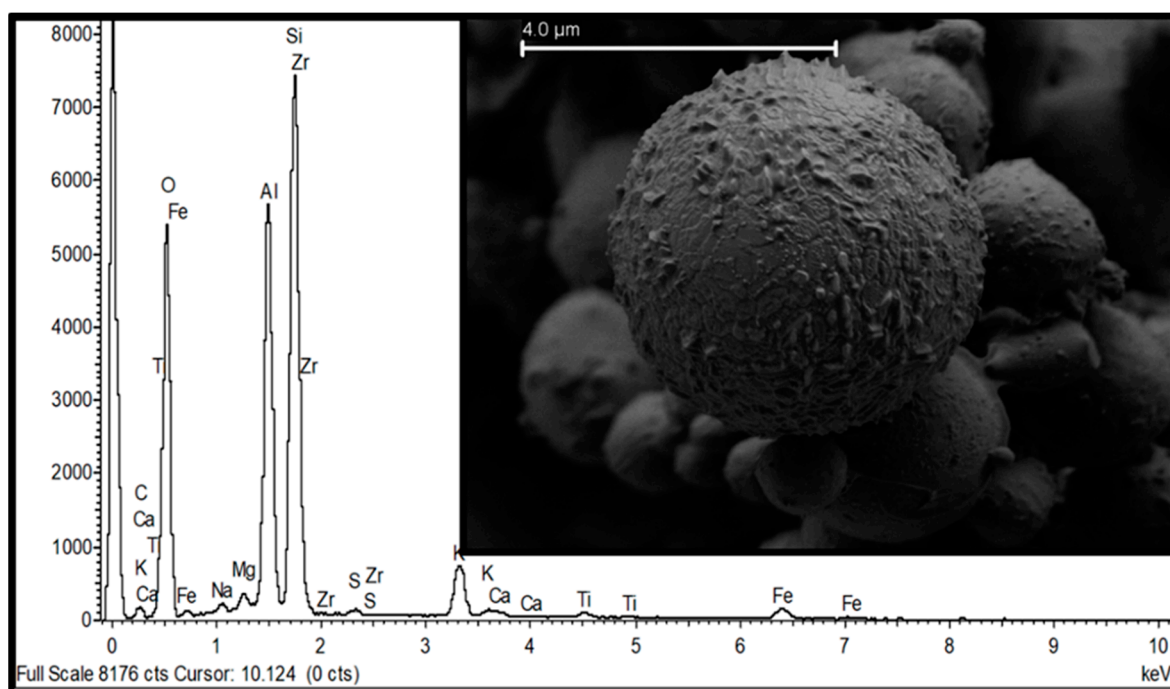


Figure 4. Detected spheres in CAC composed of Al–Ca–Fe–Mg–Si–Zr.

These thermo-geochemical conversions lead to the melting of carbon inorganic matter inclusions. Furthermore, external components with inorganic matter can present thermo-geochemical inversions when related to elements of oxidizing origin [65], with elements containing Fe and droplets.

The results of the analyzed electron beam showed that the iron spheres depend on the linear concentrations of Al, Ca, Mg and Si. In this comparison, in relation to the presence of iron, after burning coal [70] there may be variations in relation to the variability of ultrafine particles. The Fe rich morphotypes in the form of nanoparticles have a high brightness in BSE mode, due to the high Fe density. This enables its identification in low quantities, which were identified in the studied coal ash samples. The direct relationship between the geochemical compositions of the spherical components identified in the elements of Al–Ca–Fe–Mg–Si obtained from different types of combustion makes it possible to conclude that Fe in a spherical shape (detected spheres in CAC), agglomerates with inorganic matter present in coal minerals, forming droplets in Al, Ca, Mg and Si during the coal burning process in thermoelectric plants [69].

The geochemical composition and the presence of inorganic matter containing Fe in coal can compromise the efficiency of magnetic concentrates. When considering the high stability of the chemical elements of ultrafine TiO_2 particles in relation to the high degradability of concrete in an aquatic environment, it can be assumed that the release of amorphous nanophases and nanominerals are incorporated into the concrete that is used in civil construction, not altering its resistance. It is worth noting that, with the cooling of the droplets, after burning the coal, fusion occurs, and the Fe oxidation potential increases. The molecular construction of Fe^{2+} , when partially oxidized, becomes Fe^{3+} , with the occurrence of crystallization, in the concentrations of $\text{Fe}_x\text{O}_y\text{--Al}_2\text{O}_3\text{--SiO}_2$ and $\text{Fe}_x\text{O}_y\text{--CaO}$. These two phase compositions of the Fe spheres originated from the fusion of ultrafine chemical elements, due to their ease in forming reactions with each other [69].

This study identified the presence of Al–Ca–Fe–Mg–Si in the coal ash fractions, by the spherical shape of their molecular structure. Generally, the spherical structure of Fe is highly reflective, when identified in microscopy with reflected white light, where it is possible to identify Fe molecules, in magnetite and hematite phases [68]. In this relationship, the Fe spheres in ultrathin shapes were classified, considering their Fe content state and

oxidation state while observing their three dimensional surface, based on the detection of molecular electrons in the secondary structures in FE-SEM.

Through the results obtained in the ash samples, after burning, the formation of Fe can be seen in spherical structures, in geochemical and morphological phases, with the identification of macroporous surfaces, related to high (FeO–SiO₂–Al₂O₃) and low viscosities (FeO–CaO). These high Fe spheres, after combustion, represent different values in areas with specific surfaces, forming a molecular structure of microporosity in the globules.

In this study, it was found that the existence of heterogeneity in the molecular composition of individual globules, in relation to different temperatures applied during the coal burning process, resulted in different types of geomorphology. This could explain the presence of spherical globules in narrow fractions in these molecular structures of Fe. The analyses carried out on the CAC samples and tailings of coal ash from thermoelectric power plants in Santa Catarina (Brazil), which potentialize high risks to human health, consisted of ultrafine Fe particles (size 0.01–10 μm) in spherical shapes and porosities on the surface, where the vitreous aluminosilicate in the chemical element Fe stands out (Figures 3A and 4). The pseudoplero ferrospheres, since glassy spheres are filled by nano/micrometric sized coal ash, are referred to as pseudoplero spheres. It can be highlighted that, during the collection of coal ash, large open particles enabled the coupling in the pores with smaller ultrafine particles [68]. The analytical methods used for the characterization of nanominerals and amorphous nanophase present in cement are currently very limited and very low concentrations cannot be detected in complex media. This study becomes a great challenge, as it provides a description of nanomineral release, with potential to be inserted in the manufacture of nanoproducts, with a long life cycle, as is the case with concrete. However, the harmfulness of ultrafine particles to human health is highlighted.

4. Conclusions

It is known that the use of CFA for the manufacture of concrete for civil construction can achieve satisfactory results in terms of reusing and harnessing a commonly produced waste stream. However, the disregard for human health becomes evident in this manuscript, requiring more in depth studies that can highlight the harmful effects of nanoparticles on the health of workers involved in the manufacture of concrete.

It is necessary to reinforce public policies for recycling and supplying CFA on a global level in order to ensure the sustainable management of CFA sent to industries responsible for concrete manufacturing. This study identified iron, and the following hazardous elements in the CFA analyzed: Al, Ca, Mg and Si, all of which can directly harm human health.

For a more accurate quantification of the contents of CFA, this study made it possible to provide some information needed to design safety policies aimed at limiting or preventing the release of nanominerals and amorphous nanocompounds during the manufacture of concrete. The authors suggest a focus for future studies on research that will evaluate the variations in the strength of concrete utilizing coal fly ash in different concentrations and/or mixtures, with dosages to be recommended for engineers and architects working in the civil construction area.

Author Contributions: Conceptualization, A.N.; data curation, G.L.D.; formal analysis, D.P.; funding acquisition, A.N.; investigation, B.A.; project administration, D.P.; supervision, G.L.D.; visualization, A.N.; writing—original draft preparation, A.N.; writing—review and editing, G.L.D. and B.A. All authors have read and agreed to the published version of the manuscript.

Funding: This research received no external funding.

Institutional Review Board Statement: Not applicable.

Informed Consent Statement: Informed consent was obtained from all subjects involved in the study.

Data Availability Statement: Not applicable.

Acknowledgments: The authors gratefully acknowledge the NOAA Air Resources Laboratory (ARL) for the provision of the HYSPLIT transport and dispersion model and/or READY website (<http://www.ready.noaa.gov> (accessed on 11 November 2021)) used in this publication. We also wish to thank the Center for Studies and Research on Urban Mobility (NEPMOUR/IMED) and the Scientific Research Institute (Instituto de Investigación Científica, IDIC) of the University of Lima and Air Centre for supporting this research. Additionally, the National Council for Scientific and Technological Development (CNPq) for the research productivity ball in Brazil.

Conflicts of Interest: The authors declare no conflict of interest.

References

1. MME—Ministry of Mines and Energy, BRAZIL, National Energy Matrix—2030. 2019. Available online: <http://antigo.mme.gov.br/pt/web/guest/secretarias/planejamento-e-desenvolvimento-energetico/publicacoes/matriz-energetica-nacional-2030> (accessed on 12 November 2021).
2. ANEEL—National Electric Energy Agency. 2021. Available online: <https://www.aneel.gov.br> (accessed on 13 November 2021).
3. Querol, X.; Moreno, N.; Umaña, J.C.; Alastuey, A.; Hernández, E.; López-Soler, A.; Plana, F. Synthesis of zeolites from coal fly ash: An overview. *Int. J. Coal Geol.* **2002**, *50*, 413–423. [[CrossRef](#)]
4. Martinello, K.; Oliveira, M.L.S.; Molossi, F.A.; Ramos, C.G.; Teixeira, E.C.; Kautzmann, R.M.; Silva, L.F.O. Direct identification of hazardous elements in ultra-fine and nanominerals from coal fly ash produced during diesel co-firing. *Sci. Total Environ.* **2014**, *470*, 444–452. [[CrossRef](#)] [[PubMed](#)]
5. Lee, Y.R.; Soe, J.T.; Zhang, S.; Ahn, J.W.; Park, M.B.; Ahn, W.S. Synthesis of nanoporous materials via recycling coal fly ash and other solid wastes: A mini review. *Chem. Eng. J.* **2017**, *317*, 821–843. [[CrossRef](#)]
6. Kikuchi, R. Application of coal ash to environmental improvement. *Resour. Conserv. Recycl.* **1999**, *27*, 333–346. [[CrossRef](#)]
7. Teixeira, E.R.; Mateus, R.; Camões, A.F.; Bragança, L.; Branco, F.G. Comparative environmental life-cycle analysis of concretes using biomass and coal fly ashes as partial cement replacement material. *J. Clean. Prod.* **2016**, *112*, 2221–2230. [[CrossRef](#)]
8. Liu, Y.; Lu, C.P.; Zhang, H.; Wang, H.Y. Numerical investigation of slip and fracture instability mechanism of coal- rock parting-coal structure (CRCS). *J. Struct. Geol.* **2019**, *118*, 265–278. [[CrossRef](#)]
9. Hossain, M.d.U.; Dong, Y.; Ng, S.T. Influence of supplementary cementitious materials in sustainability performance of concrete industry: A case study in Hong Kong. *Case Stud. Constr. Mater.* **2021**, *15*, e00659. [[CrossRef](#)]
10. Mozgawa, W.; Król, M.; Dyzek, J.; Deja, J. Investigation of the coal fly ashes using IR spectroscopy. *Spectrochim. Acta Part A Mol. Biomol. Spectrosc.* **2014**, *132*, 889–894. [[CrossRef](#)]
11. Ahmed, S.; Arocho, I. Analysis of cost comparison and effects of change orders during construction: Study of a mass timber and a concrete building project. *J. Build. Eng.* **2021**, *33*, 101856. [[CrossRef](#)]
12. Harihanandh, M.; Viswanathan, K.; Krishnaraja, A. Comparative study on chemical and morphology properties of nano fly ash in concrete. *Mater. Today Proc.* **2021**, *45*, 3132–3136. [[CrossRef](#)]
13. Ribeiro, J.; DaBoit, K.; Flores, D.; Kronbauer, M.A.; Silva, L.F. Extensive FE-SEM/EDS, HR-TEM/EDS and ToF-SIMS studies of micron- to nano-particles in anthracite fly ash. *Sci. Total Environ.* **2013**, *452*, 98–107. [[CrossRef](#)] [[PubMed](#)]
14. Babu, K.; Nageswara Rao, G. Efficiency of fly ash in concrete. *Cem. Concr. Compos.* **1993**, *15*, 223–229. [[CrossRef](#)]
15. Colangelo, F.; Messina, F.; Palma, L.d.; Cioffi, R. Recycling of non-metallic automotive shredder residues and coal fly-ash in cold-bonded aggregates for sustainable concrete. *Compos. Part B Eng.* **2017**, *116*, 46–52. [[CrossRef](#)]
16. Silva, L.F.O.; Boit, K.M.d. Nanominerals and nanoparticles in feed coal and bottom ash: Implications for human health effects. *Environ. Monit. Assess.* **2010**, *174*, 187–197. [[CrossRef](#)]
17. Banfield, J.F.; Zhang, H. Nanoparticles in the Environment. *Rev. Mineral. Geochem.* **2001**, *44*, 1–58. [[CrossRef](#)]
18. Oliveira, M.L.S.; Ward, C.R.; Sampaio, C.H.; Querol, X.; Cutruneo, C.M.N.L.; Taffarel, S.R.; Silva, L.F.O. Partitioning of mineralogical and inorganic geochemical components of coals from Santa Catarina, Brazil, by industrial beneficiation processes. *Int. J. Coal Geol.* **2013**, *116*, 75–92. [[CrossRef](#)]
19. Silva, L.F.O.; Pinto, D.; Neckel, A.; Dotto, G.L.; Oliveira, M.L.S. The impact of air pollution on the rate of degradation of the fortress of Florianópolis Island, Brazil. *Chemosphere* **2020**, *251*, 126838. [[CrossRef](#)]
20. Oliveira, M.L.S.; Flores, E.M.M.; Dotto, G.L.; Neckel, A.; Silva, L.F.O. Nanomineralogy of mortars and ceramics from the Forum of Caesar and Nerva (Rome, Italy): The protagonist of black crusts produced on historic buildings. *J. Clean. Prod.* **2021**, *278*, 123982. [[CrossRef](#)]
21. Trejos, E.M.; Silva, L.F.O.; Hower, J.C.; Flores, E.M.M.; González, C.M.; Pachón, J.E.; Aristizábal, B.H. Volcanic emissions and atmospheric pollution: A study of nanoparticles. *Geosci. Front.* **2021**, *12*, 746–755. [[CrossRef](#)]
22. Silva, L.F.O.; Moreno, T.; Querol, X. An introductory TEM study of Fe-nanominerals within coal fly ash. *Sci. Total Environ.* **2009**, *407*, 4972–4974. [[CrossRef](#)]
23. Quispe, D.; Pérez-López, R.; Silva, L.F.O.; Nieto, J.M. Changes in mobility of hazardous elements during coal combustion in Santa Catarina power plant (Brazil). *Fuel* **2012**, *94*, 495–503. [[CrossRef](#)]

24. Cutruneo, C.M.N.L.; Oliveira, M.L.S.; Ward, C.R.; Hower, J.C.; Brum, I.A.S.d.; Sampaio, C.H.; Kautzmann, R.M.; Taffarel, S.R.; Teixeira, E.C.; Silva, L.F.O. A mineralogical and geochemical study of three Brazilian coal cleaning rejects: Demonstration of electron beam applications. *Int. J. Coal Geol.* **2014**, *130*, 33–52. [[CrossRef](#)]
25. Cerqueira, B.; Vega, F.A.; Serra, C.; Silva, L.F.O.; Andrade, M.L. Time of flight secondary ion mass spectrometry and high-resolution transmission electron microscopy/energy dispersive spectroscopy: A preliminary study of the distribution of Cu²⁺ and Cu²⁺/Pb²⁺ on a BT horizon surfaces. *J. Hazard. Mater.* **2011**, *195*, 422–431. [[CrossRef](#)] [[PubMed](#)]
26. Silva, L.F.O.; Hower, J.; Izquierdo, M.; Querol, X. Complex nanominerals and ultrafine particles assemblages in phosphogypsum of the fertilizer industry and implications on human exposure. *Sci. Total Environ.* **2010**, *408*, 5117–5122. [[CrossRef](#)] [[PubMed](#)]
27. Silva, L.F.O.; Jasper, A.; Andrade, M.L.; Sampaio, C.H.; Dai, S.; Li, X.; Li, T.; Chen, W.; Wang, X.; Liu, H.; et al. Applied investigation on the interaction of hazardous elements binding on ultrafine and nanoparticles in Chinese anthracite-derived fly ash. *Sci. Total Environ.* **2012**, *419*, 250–264. [[CrossRef](#)] [[PubMed](#)]
28. Silva, L.F.O.; Oliveira, M.L.S.; Sampaio, C.H.; De Brum, I.A.S.; Hower, J.C. Vanadium and nickel speciation in pulverized coal and petroleum coke co-combustion. *Energy Fuels* **2013**, *27*, 1194–1203. [[CrossRef](#)]
29. Ramos, C.G.; Querol, X.; Oliveira, M.L.S.; Pires, K.; Kautzmann, R.M.; Silva, L.F. A preliminary evaluation of volcanic rock powder for application in agriculture as soil a remineralizer. *Sci. Total Environ.* **2015**, *512*, 371–380. [[CrossRef](#)]
30. Schneider, I.L.; Teixeira, E.C.; Silva, L.F.O.; Wiegand, F. Atmospheric particle number concentration and size distribution in a traffic-impacted area. *Atmos. Pollut. Res.* **2015**, *6*, 877–885. [[CrossRef](#)]
31. Wilcox, J.; Wang, B.; Rupp, E.; Taggart, R.; Hsu-Kim, H.; Oliveira, M.; Cutruneo, C.; Taffarel, S.; Silva, L.F.; Hopps, S.; et al. Observations and assessment of fly ashes from high-sulfur bituminous coals and blends of high-sulfur bituminous and subbituminous coals: Environmental processes recorded at the macro and nanometer scale. *Energy Fuels* **2015**, *29*, 7168–7177. [[CrossRef](#)]
32. Civeira, M.S.; Ramos, C.G.; Oliveira, M.L.S.; Kautzmann, R.M.; Taffarel, S.R.; Teixeira, E.C.; Silva, L.F. Nano-mineralogy of suspended sediment during the beginning of coal rejects spill. *Chemosphere* **2016**, *145*, 142–147. [[CrossRef](#)]
33. Dalmora, A.C.; Ramos, C.G.; Querol, X.; Kautzmann, R.M.; Oliveira, M.L.S.; Taffarel, S.R.; Moreno, T.; Silva, L.F. Nanoparticulate mineral matter from basalt dust wastes. *Chemosphere* **2016**, *144*, 2013–2017. [[CrossRef](#)] [[PubMed](#)]
34. Dalmora, A.C.; Ramos, C.; Oliveira, M.; Teixeira, E.; Kautzmann, R.; Taffarel, S.; De Brum, I.; Silva, L.F. Chemical characterization, nano-particle mineralogy and particle size distribution of basalt dust wastes. *Sci. Total Environ.* **2016**, *539*, 560–565. [[CrossRef](#)] [[PubMed](#)]
35. León-Mejía, G.; Silva, L.F.O.; Civeira, M.S.; Da Silva, J.; Henriques, J.A.P. Cytotoxicity and genotoxicity induced by coal and coal fly ash particles samples in V79 cells. *Environ. Sci. Pollut. Res.* **2016**, *23*, 24019–24031. [[CrossRef](#)] [[PubMed](#)]
36. Rodríguez-Iruretagoiena, A.; De Vallejuelo, S.; De Diego, A.; De Leão, F.; De Medeiros, D.; Oliveira, M.; Taffarel, S.; Arana, G.; Madariaga, J.; Silva, L.F. The mobilization of hazardous elements after a tropical storm event in a polluted estuary. *Sci. Total Environ.* **2016**, *565*, 721–729. [[CrossRef](#)] [[PubMed](#)]
37. Sehn, J.; De Leão, F.; Da Boit, K.; Oliveira, M.; Hidalgo, G.; Sampaio, C.; Silva, L.F. Nanomineralogy in the real world: A perspective on nanoparticles in the environmental impacts of coal fire. *Chemosphere* **2016**, *147*, 439–443. [[CrossRef](#)]
38. Dutta, M.; Saikia, J.; Taffarel, S.R.; Waanders, F.B.; De Medeiros, D.; Cutruneo, C.M.; Saikia, B.K. Environmental assessment and nano-mineralogical characterization of coal, overburden and sediment from Indian coal mining acid drainage. *Geosci. Front.* **2017**, *8*, 1285–1297. [[CrossRef](#)]
39. Sánchez-Peña, N.E.; Narváez-Semanate, J.L.; Pabón-Patiño, D.; Fernández-Mera, J.E.; Oliveira, M.L.; Da Boit, K.; Tutikian, B.; Crissien, T.; Pinto, D.; Serrano, I.; et al. Chemical and nano-mineralogical study for determining potential uses of legal Colombian gold mine sludge: Experimental evidence. *Chemosphere* **2018**, *191*, 1048–1055. [[CrossRef](#)]
40. León-Mejía, G.; Machado, M.N.; Okuro, R.T.; Silva, L.F.; Telles, C.; Dias, J.; Niekraszewicz, L.; Da Silva, J.; Henriques, J.A.P.; Zin, W.A. Intratracheal instillation of coal and coal fly ash particles in mice induces DNA damage and translocation of metals to extrapulmonary tissues. *Sci. Total Environ.* **2018**, *625*, 589–599. [[CrossRef](#)]
41. Nordin, A.P.; Da Silva, J.; De Souza, C.; Niekraszewicz, L.A.B.; Dias, J.F.; Da Boit, K.; Oliveira, M.L.S.; Grivicich, I.; Garcia, A.L.; Silva, L.F.; et al. In vitro genotoxic effect of secondary minerals crystallized in rocks from coal mine drainage. *J. Hazard. Mater.* **2018**, *346*, 263–272. [[CrossRef](#)]
42. Silva, L.F.O.; Pinto, D.; Neckel, A.; Oliveira, M.L.S.; Sampaio, C.H. Atmospheric nanocompounds on Lanzarote Island: Vehicular exhaust and igneous geologic formation interactions. *Chemosphere* **2020**, *254*, 126822. [[CrossRef](#)]
43. Silva, L.F.O.; Pinto, D.; Neckel, A.; Oliveira, M.L.S. An analysis of vehicular exhaust derived nanoparticles and historical Belgium fortress building interfaces. *Geosci. Front.* **2020**, *11*, 2053–2060. [[CrossRef](#)]
44. Lima, B.D.; Teixeira, E.C.; Hower, J.C.; Civeira, M.S.; Ramírez, O.; Yang, C.; Oliveira, M.L.S.; Silva, L.F.O. Metal-enriched nanoparticles and black carbon: A perspective from the Brazil railway system air pollution. *Geosci. Front.* **2021**, *12*, 101129. [[CrossRef](#)]
45. Neckel, A.; Oliveira, M.L.S.; Bolaño, L.J.C.; Maculan, L.S.; Moro, L.; Bodah, E.T.; Moreno-Ríos, A.L.; Bodah, B.W.; Silva, L.F. Biophysical matter in a marine estuary identified by the Sentinel-3B OLCI satellite and the presence of terrestrial iron (Fe) nanoparticles. *Mar. Pollut. Bull.* **2021**, *173*, 112925. [[CrossRef](#)] [[PubMed](#)]
46. Oliveira, M.L.; Neckel, A.; Silva, L.F.; Dotto, G.L.; Maculan, L.S. Environmental aspects of the depreciation of the culturally significant Wall of Cartagena de Indias—Colombia. *Chemosphere* **2021**, *265*, 129119. [[CrossRef](#)] [[PubMed](#)]

47. Ravindra Babu, S.; Nguyen, L.S.P.; Sheu, G.R.; Griffith, S.M.; Pani, S.K.; Huang, H.Y.; Lin, N.H. Long-range transport of La Soufrière volcanic plume to the western North Pacific: Influence on atmospheric mercury and aerosol properties. *Atmos. Environ.* **2022**, *268*, 118806. [[CrossRef](#)]
48. Zhu, Q.; Li, J.; Li, G.; Wen, S.; Yu, R.; Tang, C.; Feng, X.; Liu, X. Characteristics of Sandstone-type Uranium Mineralization in the Hangjinqi Region of the Northeastern Ordos Basin: Clues from Clay Mineral Studies. *Ore Geol. Rev.* **2021**, *141*, 104642. [[CrossRef](#)]
49. Zeng, S.; Shen, Y.; Sun, B.; Zhang, N.; Zhang, S.; Feng, S. Pore structure evolution characteristics of sandstone uranium ore during acid leaching. *Nucl. Eng. Technol.* **2021**, *53*, 4033–4041. [[CrossRef](#)]
50. Yue, L.; Jiao, Y.; Fayek, M.; Wu, L.; Rong, H. Micromorphologies and sulfur isotopic compositions of pyrite in sandstone-hosted uranium deposits: A review and implications for ore genesis. *Ore Geol. Rev.* **2021**, *139*, 104512. [[CrossRef](#)]
51. Zhang, J.; Cheng, J.C.P.; Lo, I.M.C. Life cycle carbon footprint measurement of Portland cement and ready mix concrete for a city with local scarcity of resources like Hong Kong. *Int. J. Life Cycle Assess.* **2014**, *19*, 745–757. [[CrossRef](#)]
52. Rafieizonooz, M.; Mirza, J.; Salim, M.R.; Hussin, M.W.; Khankhaje, E. Investigation of coal bottom ash and fly ash in concrete as replacement for sand and cement. *Constr. Build. Mater.* **2016**, *116*, 15–24. [[CrossRef](#)]
53. Gao, Z.F.; Long, H.M.; Dai, B.; Gao, X.P. Investigation of reducing particulate matter (PM) and heavy metals pollutions by adding a novel additive from metallurgical dust (MD) during coal combustion. *J. Hazard. Mater.* **2019**, *373*, 335–346. [[CrossRef](#)] [[PubMed](#)]
54. Oliveira, M.L.S.; Ward, C.R.; Izquierdo, M.; Sampaio, C.H.; Brum, I.A.S.d.; Kautzmann, R.M.; Sabedot, S.; Querol, X.; Silva, L.F.O. Chemical composition and minerals in pyrite ash of an abandoned sulphuric acid production plant. *Sci. Total Environ.* **2012**, *430*, 34–47. [[CrossRef](#)] [[PubMed](#)]
55. Oliveira, M.L.S.; Ward, C.R.; French, D.; Hower, J.C.; Querol, X.; Silva, L.F.O. Mineralogy and leaching characteristics of beneficiated coal products from Santa Catarina, Brazil. *Int. J. Coal Geol.* **2012**, *94*, 314–325. [[CrossRef](#)]
56. Mench, M.; Lepp, N.; Bert, V.; Schwitzguébel, J.P.; Gawronski, S.W.; Schröder, P.; Vangronsveld, J. Successes and limitations of phytotechnologies at field scale: Outcomes, assessment and outlook from cost action 859. *J. Soils Sediments* **2010**, *10*, 1039–1070. [[CrossRef](#)]
57. Lee, S.H.; Lee, J.S.; Choi, Y.J.; Kim, J.G. In situ stabilization of cadmium-, lead-, and zinc-contaminated soil using various amendments. *Chemosphere* **2009**, *77*, 1069–1075. [[CrossRef](#)]
58. Šaltauskaitė, J.; Kniuipytė, I.; Praspaliauskas, M. Earthworm *Eisenia fetida* potential for sewage sludge amended soil valorization by heavy metal remediation and soil quality improvement. *J. Hazard. Mater.* **2022**, *424*, 127316. [[CrossRef](#)]
59. He, J.; Cai, Y.; Lv, J.; Zhang, L. Primary investigation of quartz as a possible carcinogen in coals of Xuanwei and Fuyuan, high lung cancer incidence area in China. *Environ. Earth Sci.* **2012**, *67*, 1679–1684. [[CrossRef](#)]
60. Downward, G.S.; Hu, W.; Rothman, N.; Reiss, B.; Tromp, P.; Wu, G.; Wei, F.; Xu, J.; Seow, W.J.; Chapman, R.S. Quartz in ash, and air in a high lung cancer incidence area in China. *Environ. Pollut.* **2017**, *221*, 318–325. [[CrossRef](#)]
61. Downward, G.S.; Hu, W.; Rothman, N.; Reiss, B.; Wu, G.; Wei, F.; Chapman, R.S.; Portengen, L.; Qing, L.; Vermeulen, R. Polycyclic Aromatic Hydrocarbon Exposure in Household Air Pollution from Solid Fuel Combustion among the Female Population of Xuanwei and Fuyuan Counties, China. *Environ. Sci. Technol.* **2014**, *48*, 14632–14641. [[CrossRef](#)]
62. Onchoke, K.K. ¹³C NMR chemical shift assignments of nitrated benzo[a]pyrenes based on two-dimensional techniques and DFT/GIAO calculations. *Results Chem.* **2021**, *3*, 100099. [[CrossRef](#)]
63. Navarrete, I.; Vargas, F.; Martinez, P.; Paul, A.; Lopez, M. Flue gas desulfurization (FGD) fly ash as a sustainable, safe alternative for cement-based materials. *J. Clean. Prod.* **2021**, *283*, 124646. [[CrossRef](#)]
64. Ramakrishnan, K.; Depak, S.R.; Hariharan, K.R.; Abid, S.R.; Murali, G.; Cecchin, D.; Fediuk, R.; Amran, Y.H.M.; Abdelgader, H.S.; Khatib, J.M. Standard and modified falling mass impact tests on replaced aggregate fibrous concrete and slurry infiltrated fibrous concrete. *Constr. Build. Mater.* **2021**, *298*, 123857. [[CrossRef](#)]
65. Zhao, Y.; Zhang, J.; Sun, J.; Bai, X.; Zheng, C. Mineralogy, Chemical Composition, and Microstructure of Ferrospheres in Fly Ashes from Coal Combustion. *Energy Fuels* **2006**, *20*, 1490–1497. [[CrossRef](#)]
66. Strzałkowska, E. Morphology, chemical and mineralogical composition of magnetic fraction of coal fly ash. *Int. J. Coal Geol.* **2021**, *240*, 103746. [[CrossRef](#)]
67. Matjie, R.H.; French, D.; Ward, C.R.; Pistorius, P.C.; Li, Z. Behaviour of coal mineral matter in sintering and slagging of ash during the gasification process. *Fuel Process. Technol.* **2011**, *92*, 1426–1433. [[CrossRef](#)]
68. Valentim, B.; Shreya, N.; Paul, B.; Gomes, C.S.; Sant’ovaia, H.; Guedes, A.; Ribeiro, J.; Flores, D.; Pinho, S.; Suárez-Ruiz, I. Characteristics of ferrospheres in fly ashes derived from Bokaro and Jharia (Jharkand, India) coals. *Int. J. Coal Geol.* **2016**, *153*, 52–74. [[CrossRef](#)]
69. Sharonova, O.M.; Anshits, N.N.; Solovyov, L.A.; Salanov, A.N.; Anshits, A.G. Relationship between composition and structure of globules in narrow fractions of ferrospheres. *Fuel* **2013**, *111*, 332–343. [[CrossRef](#)]
70. Vassilev, S.V.; Menendez, R.; Borrego, A.G.; Diaz-Somoano, M.; Martinez-Tarazona, M.R. Phase-mineral and chemical composition of coal fly ashes as a basis for their multicomponent utilization. 3. Characterization of magnetic and char concentrates. *Fuel* **2004**, *83*, 1563–1583. [[CrossRef](#)]